

National and Kapodistrian University of Athens

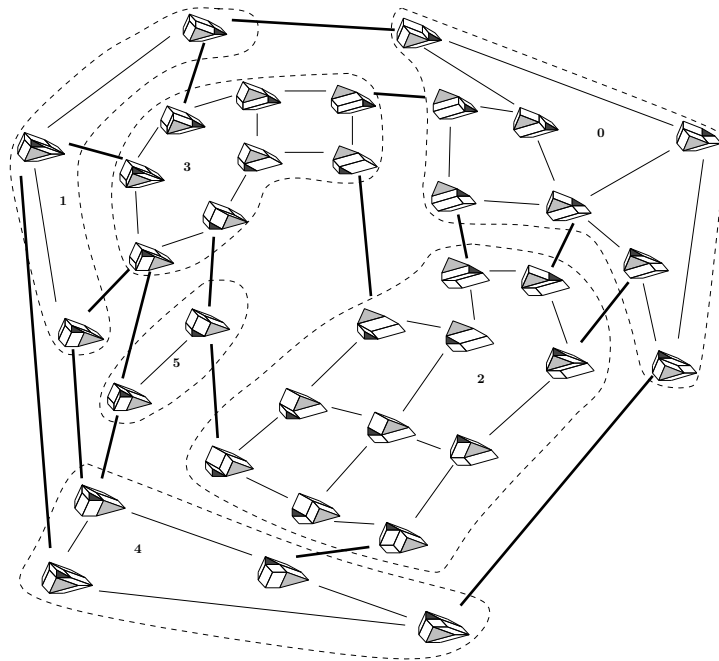
M.Sc. Thesis

Graduate Program in Logic, Algorithms and Computation

$\mu\text{Π}\lambda\forall$

Triangulations of point sets, high dimensional Polytopes and Applications

Vissarion Fisikopoulos



Supervised by
Prof. Ioannis Z. Emiris

Athens, March 2010

Introduction

In this thesis we are interested in algorithms that compute the Newton polytope of the Resultant, called *Resultant polytope*, of a given set of polynomial equations. Resultants are fundamental objects in polynomial equation solving and in implicitizing parametric (hyper)surfaces; see, e.g., [DE05, EK05]. In fact, a projection of the resultant polytope yields the Newton polytope of the (unknown) implicit equation, thus reducing implicitization to a problem in linear algebra. One approach, in which we will like to focus, is to compute the *regular fine mixed subdivisions* of the Minkowski sum of the supports of the given equations. Another is based on tropical geometry [SY08].

The input is the support point sets of the given equations. The regular fine mixed subdivisions of the Minkowski sum of these point sets correspond, by *Cayley's trick*, to the regular triangulations of a new point set A constructed by these point sets. For each point set A , there is a polytope, named *secondary polytope*, whose vertices correspond to the regular triangulations of A and there are output-sensitive algorithms that enumerate them [MII96, PR03]. Thus, we can compute all regular fine mixed subdivisions of the Minkowski sum of the input support point sets by enumerating the regular triangulations of another point set using Cayley trick and enumeration algorithms for regular triangulations. However, the number of vertices of a secondary polytope can be exponential in $|A|$ and there is a many to one correspondence of secondary vertices to the vertices of the Resultant polytope. Therefore this computation could be inefficient. This basic observation is illustrated by the experiments of this thesis also presented in [Fis09]. On the other hand, for the resultant polytope, we only know a weak exponential upper bound on the number of vertices [Stu94, prop.6.1].

As a next step, we study classes of regular fine mixed subdivisions, called *i -mixed cell configurations*. [Kon06] present an enumeration algorithm of all these configurations. Although using this algorithm to compute the Resultant polytope is more efficient than enumerating the entire secondary polytope this method is far from the optimal enumeration of the Resultant polytope. The above results force us to focus on output-sensitive algorithms

that enumerate classes of subdivisions which yield the same resultant vertex. In this thesis we present an algorithmic characterization of secondary edges, called *cubical flips*, which connect two such classes and we show that these edges does not suffice to enumerate the Resultant polytope. Some results of this thesis have been published in [EFK10].

In the first chapter we present the fundamental notions needed. Algorithms that enumerate regular triangulations are also discussed. The second chapter introduce the mixed cell configurations, Ξ polytopes and cubical flips. It is discussed how these can be used to optimize the computation of the Resultant polytope. Finally, in the third chapter we present an application of these algorithms to an implicitization algorithm. We also present experimental results of this algorithm on well-known curves and surfaces and discuss future work.

Acknowledgments

First and foremost, I would like to thank my supervisor Ioannis Emiris for his patient guidance and advice, and his belief in me throughout my time as his student and particularly during the writing of this thesis. I would also like to thank the other two members of my Advisory Committee, namely Elias Koutsoupias and Dimitrios Gounopoulos for the helpful discussions and support on my thesis subject.

Moreover, I'd like to thank all the members of $E\rho\Gamma A$ lab, namely George, Zafirakis, Christos S., Tatjana, Elias, Antonis, Angelos for the friendly working environment and especially Cristos K. for his continuous assistance on my thesis work. I would also like to thank very much Fumihiko Takeuchi for running some useful experiments for me and Monique Teillaud for the useful discussions.

Finally, I would like to thank my parents and my brother for their everyday support on my choices. I also feel the need to thank my friends for their understanding and patience throughout the last years when my free time for them was limited. Last but not least, I must express my gratitude to Sofia for her unconditional support and encouragement.

Typesetting

This document was typesetted on \LaTeX . All figures are created with the extensible drawing editor Ipe (<http://ipe7.sourceforge.net>).

Vissarion Fisikopoulos
Athens, March 2010

1	Triangulations, mixed subdivisions, and polynomial systems	1
1.1	Polyhedral subdivisions	1
1.2	Mixed subdivisions	5
1.3	The Resultant polytope	6
1.4	Enumeration algorithms	8
2	Mixed cell configurations and R-equivalent classes	13
2.1	Mixed cell configurations	13
2.2	R-equivalent classes	18
3	Experiments, applications and conclusions	23
3.1	Implicitization	23
3.2	Experiments - Software	24
3.3	An example: the equation of circle	27
3.4	Conclusions and future work	30
	Bibliography	33
	Index	37
	List of Figures	38

CHAPTER 1

Triangulations, mixed subdivisions, and polynomial systems

This chapter is an introduction to some fundamental notions and tools which are used in this thesis. The first one covers triangulations of point sets and introduce one basic tool; the secondary polytopes. The second part introduce mixed subdivisions and their connection to triangulations via Cayley trick. In the third part we present the central problem of this thesis the computation of the Resultant polytope of a system of polynomial equations using as tools enumeration algorithms for secondary polytopes and the Cayley trick. In the last part we focus on two approaches for enumeration of secondary polytopes. To conclude with, the theory of this chapter yields an algorithm that compute the Resultant polytope. This is the algorithm we will try to optimize in next chapters. A nice introduction to triangulations of point sets and secondary polytopes is [LRS08] as well as [Zie95] to polytope theory.

1.1 Polyhedral subdivisions

Let $A = a_1, a_1, \dots, a_m$ a point set in \mathbb{R}^d . A *face* of A is a subset of A where a certain linear function is maximized. Faces of dimension $0, 1, d-2, d-1$ are called vertices, edges, ridges and facets respectively. We will denote $\text{conv}(A)$ the *convex hull* of A . A *simplex* of A is an affinely independent subset of A .

Definition 1.1.1. (Polyhedral Subdivision) A *polyhedral subdivision* of A is a collection S of subsets of A called cells such that

- Union Property (UP): $\cup_{\sigma \in S} \text{conv}(\sigma) = \text{conv}(A)$
- Intersection Property (IP): $\forall \sigma, \tau \in S, \text{conv}(\sigma \cap \tau) = \text{conv}(\sigma) \cap \text{conv}(\tau)$ and $\sigma \cap \tau$ is a face of both $\text{conv}(\sigma), \text{conv}(\tau)$

Note that not necessarily all the points of A take place in a polyhedral subdivision. Note that w can be seen as a m -dimensional vector called *volume vector*.

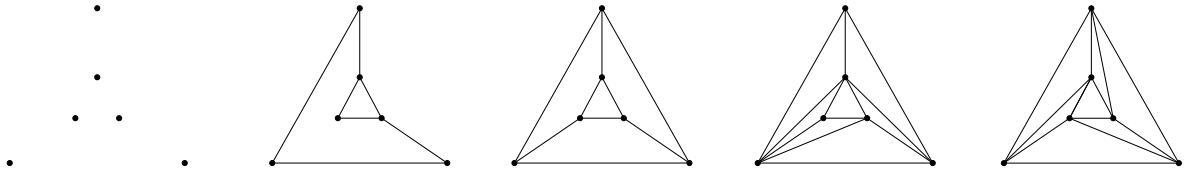


Fig. 1.1: A point set, an invalid subdivisions, a regular polyhedral subdivision, a regular triangulation and a non regular triangulation.

Let $w : A \rightarrow \mathbb{R}$ a function that lifts A from \mathbb{R}^d to \mathbb{R}^{d+1} and $\tilde{A} = (a, w(a)), a \in A$ the new lifted point set. The *lower facets* of \tilde{A} are those whose last coordinate of the exterior normal vector is negative. The *lower hull* is the set of all lower facets of $\text{conv}(\tilde{A})$.

Definition 1.1.2. (Regular Subdivision) A *regular subdivision* is the projection of the lower hull of \tilde{A} to \mathbb{R}^d ie.

$$S_r = \pi(F \cap \tilde{A}) : F \text{ the lower hull of } \tilde{A}$$

where $\pi : \mathbb{R}^{d+1} \rightarrow \mathbb{R}^d$.

For the lifting function $w(a) = \|a\|^2$ it is the Delaunay subdivision, where $\|\cdot\|$ is the Euclidean norm.

Definition 1.1.3. (Triangulation) A polyhedral subdivision of A whose cells are all simplices, is called *triangulation*.

Every regular triangulation corresponds to a volume vector. For an illustration of these notions see figure 1.1.

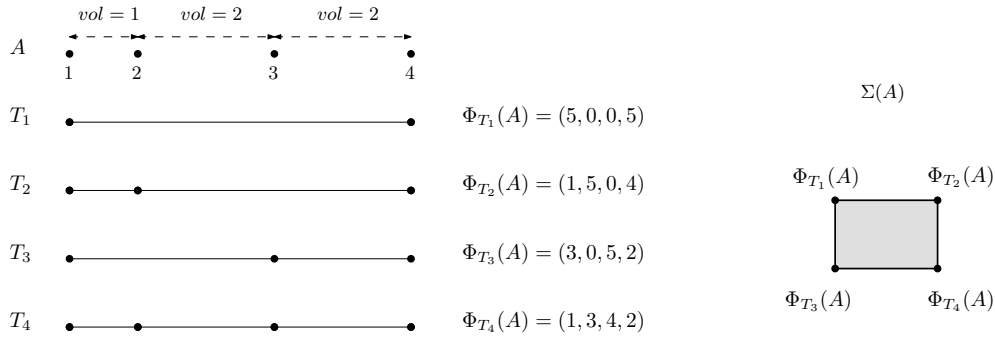
Definition 1.1.4. (GKZ-vector) Let T be a triangulation of A . Then the GKZ-vector of T is $\Phi_T(A) = (\phi_1(A), \phi_2(A), \dots, \phi_m(A))$

$$\phi_i(A) = \sum_{\sigma \in T: a_i \in \sigma} \text{vol}(\sigma)$$

where vol denotes the Euclidean volume. In other words, for each point a_i we compute the sum of the volumes of all simplices in the triangulation T which include a_i and this sum corresponds to the i -coordinate of the vector $\Phi_T(A)$.

Definition 1.1.5. (Secondary polytope) The *secondary polytope* $\Sigma(A)$ is the convex hull of GKZ-vectors for all triangulations of A .

Example 1.1.6. Assume we have the point set $A = \{1, 2, 4, 6\}$ in \mathbb{R}^1 then the GKZ vectors of all triangulations and the corresponding secondary polytope of A are as follows.



Let us now introduce the notion of *flip*, that is an operation that takes us from one triangulation to another.

Definition 1.1.7. (Circuit) A *circuit* of A is a minimal affinely dependent subset of A , i.e. it is dependent but every proper subset is independent (fig. 1.2).

Let $Z = \{z_1, \dots, z_k\}$ be a circuit; it is affinely dependent so there is an affine dependence equation and also it is minimal so this equation is unique:

$$\sum_{i \in [1, k]} \lambda_i z_i = 0, \quad \sum_{i \in [1, k]} \lambda_i = 0, \quad \lambda_i \neq 0$$

which splits Z in two subsets $Z_+ = \{z_i | \lambda_i > 0\}$ and $Z_- = \{z_i | \lambda_i < 0\}$, i.e. $Z = Z_+ \sqcup Z_-$. The partition (Z_+, Z_-) is called *oriented circuit* or *Randon partition*.

Proposition 1.1.8. ([GKZ94]) *Every circuit Z has exactly two triangulations*

$$T_Z^+ = \{Z \setminus \{z_i\} : z_i \in Z_+\} \quad T_Z^- = \{Z \setminus \{z_i\} : z_i \in Z_-\}$$

which are also regular.

A triangulation, for example T_Z^+ , is constructed in the following way; for each point $z_i \in Z_+$ we exclude it from the circuit creating a simplex; the union of all these simplices compose the triangulation. Note that: $\#simplices(T_Z^+) = |Z_+|$, the same holds for T_Z^- .

Definition 1.1.9. We will say that a triangulation T is *supported* on a circuit Z if there exist subsets F_1, F_2, \dots, F_s of A ($s \geq 1$) and a triangulation T_Z (which is either T_Z^+ or T_Z^-) of Z such that:

- $\forall I \in T_Z, \forall J \in T : (I \subset J) \Rightarrow (\exists i \in \{1, 2, \dots, s\} : J = F_i \cup I)$
- $\forall i \in \{1, 2, \dots, s\}, \forall I \in T : F_i \cup I \in T$

Definition 1.1.10. (Link) The *link* of a set $\tau \in A$ in a triangulation T of A is defined as:

$$link_T(\tau) := \{\rho \subseteq A : \rho \cap \tau = \emptyset, \rho \cup \tau \in T\}$$

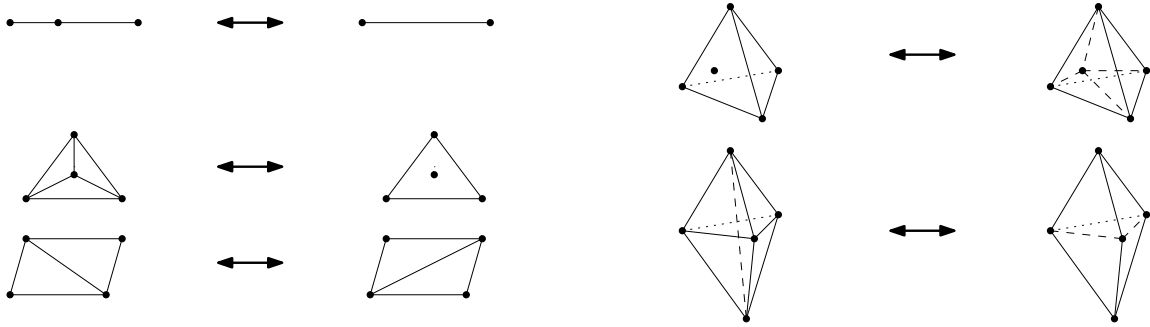


Fig. 1.2: Circuits of dimension 1,2,3 and their corresponding triangulations.

In other words, the link of a cell $\sigma \in T$ consists of the sets that we get by removing σ from the simplices that contain σ .

Definition 1.1.11. (Bistellar Flip) The operation of switching from one triangulation to another is called *bistellar flip*. More precisely, let T be a triangulation of A and Z be a circuit of A . Suppose that T contains T_Z^+ and all cells $\tau \in T_Z^+$ have the same link L in T . Then we say that Z supports a (bistellar) flip in T and a new triangulation T' of A is obtained from T by this flip.

$$T' = T \setminus \{\rho \cup \tau : \rho \in L, \tau \in T_Z^+\} \cup \{\rho \cup \tau : \rho \in L, \tau \in T_Z^-\}$$

Thus, T' is obtained from T by replacing T_Z^+ and whatever is joined to link L by T_Z^- and joining it to the same link L . We will denote this operation by $flip_Z(T)$ (fig. 1.3).

Proposition 1.1.12. (Gelfand-Kapranov-Zelevinskii [GKZ94]) *For every point set A of m points in \mathbb{R}^d corresponds a secondary polytope $\Sigma(A)$ with dimension $dim(\Sigma(A)) = m - d - 1$. The vertices correspond to the regular triangulations of A and the edges to bistellar flips between regular triangulations of A .*

Definition 1.1.13. (p -skeleton) A p -skeleton of a polytope P is a simplicial subcomplex of P that is the collection of all simplices of of dimension at most p .

The 1-skeleton of a polytope P is a graph G consisting of all vertices and edges of P .

Definition 1.1.14. (Graph of Flips) The *graph of flips* of A is a graph $G = (V, E)$ where V is the set of all triangulations of A and there is an edge $(T, T') \in E$ if and only if there is a bistellar flip from T to T' .

Note that a bistellar flip on a regular triangulation may lead to a non regular triangulation. As a result, the graph of flips and the 1-skeleton of the Secondary polytope are not the same in general.

Results on the graph of flips. It is known [Wag36] that the graph of flips for points in \mathbb{R}^2 is connected. The same problem is open for points in \mathbb{R}^3 . On the negative side, in [San06] there is a construction of points in \mathbb{R}^5 with a disconnected graph of flips. On the positive side, and also the one we are interested in, if we restrict to regular triangulations the graph of flips for points in arbitrary dimension \mathbb{R}^d is always connected [GKZ94].

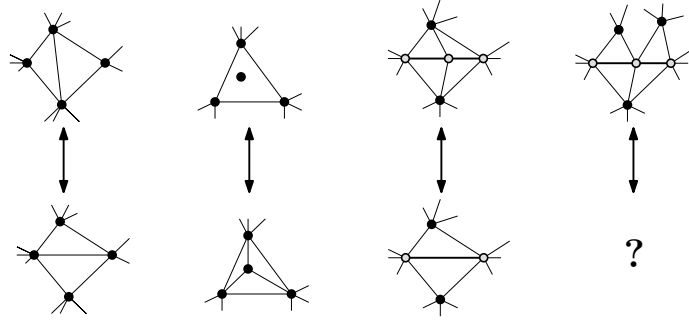


Fig. 1.3: Bistellar flips supported on full dimensional circuits (1,2) and on lower dimensional circuits (3). Link condition not satisfied in (4).

Let us conclude this section with a well-known upper bound result of convex polytopes.

Proposition 1.1.15. ([McM71]) *Let P a convex polytope in \mathbb{R}^d . The number of faces of P is $\Theta(m^{\lfloor d/2 \rfloor})$.*

A direct corollary of this result is that the number of any dimensional simplices in a regular triangulation is $O(m^{\lfloor d/2 \rfloor})$.

1.2 Mixed subdivisions

Definition 1.2.1. (Minkowski Sum) The Minkowski sum of two convex polytopes P_1 and P_2 is the convex polytope:

$$P = P_1 + P_2 := \{p_1 + p_2 \mid p_1 \in P_1, p_2 \in P_2\}$$

Let A_0, \dots, A_n be points sets in \mathbb{R}^d and $m_i = |A_i|$. Let also $\bar{A} = A_0 + \dots + A_n$ be the Minkowski sum.

Definition 1.2.2. (Minkowski Cell) A subset of \bar{A} or cell is called *Minkowski cell* if it can be written as $F_0 + \dots + F_n$ for certain subsets $F_0 \subseteq A_0, \dots, F_n \subseteq A_n$. Additionally a Minkowski cell is *fine* if all F_i are affinely independent and $\sum_{i=1}^n \dim(\text{conv}(F_i)) = d$. When $n = d$, a Minkowski cell is *i-mixed* if it is a Minkowski sum of n edges and a vertex, i.e. $|F_j| = 2$ for $j \neq i$, $|F_i| = 1$. When $n = d - 1$, a Minkowski cell is *mixed* if it is a Minkowski sum of edges i.e. all $|F_i| = 1$.

Definition 1.2.3. (Mixed Subdivision) A regular polyhedral subdivision of \bar{A} is a *regular fine mixed subdivision* if all its cells are Minkowski and fine (fig. 1.4).

Remark 1.2.4. The fine mixed subdivisions are the analogue of triangulations. The fine Minkowski cells are the analogue of simplices. Note that in the case $n = d$ ($n = d - 1$) the cells of a fine mixed subdivision are not necessarily *i-mixed* (mixed).

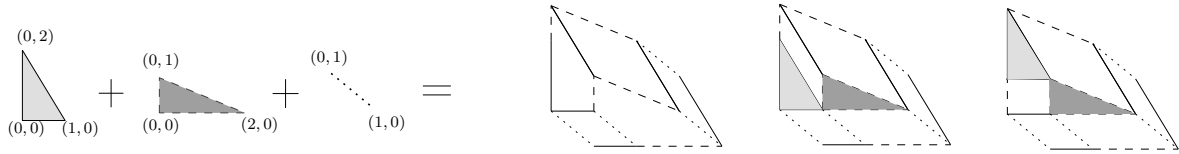


Fig. 1.4: A Minkowski sum of 2 triangles and an edge, one non fine mixed subdivision (the first) and two fine mixed subdivisions (the white cells are mixed and the grey are non mixed).

From now on we consider all mixed subdivisions to be regular and fine and focus on $n = d$, unless otherwise noted.

Definition 1.2.5. (Cayley embedding) The *Cayley embedding* of A_1, \dots, A_n is the point set $\mathcal{C}(A_1, \dots, A_n) = A_1 \times \{e_1\} \cup A_2 \times \{e_2\} \cup \dots \cup A_n \times \{e_n\} \subseteq \mathbb{R}^d \times \mathbb{R}^{n-1}$, where e_1, e_2, \dots, e_n are an affine basis of \mathbb{R}^{n-1} .

Proposition 1.2.6. (the Cayley trick [GKZ94]) *There is a bijection between polyhedral subdivisions of $\mathcal{C}(A_1, \dots, A_n)$ and mixed subdivisions of $A_1 + \dots + A_n$ which restricts to bijections between*

1. regular subdivisions of $\mathcal{C}(A_1, \dots, A_n)$ and generalized regular mixed subdivisions of $A_1 + \dots + A_n$,
2. triangulations of $\mathcal{C}(A_1, \dots, A_n)$ and (fine) mixed subdivisions of $A_1 + \dots + A_n$

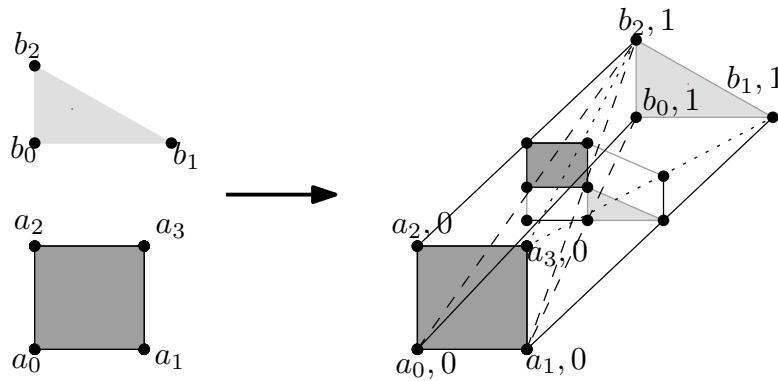


Fig. 1.5: One picture proof of Cayley trick.

By Cayley trick we get that the vertices of the secondary polytope $\Sigma(A)$, which correspond to regular triangulations, also correspond to the mixed subdivisions of A (fig. 1.5).

1.3 The Resultant polytope

Let $f = f_0, f_1, \dots, f_n$ a system of polynomials on n variables.

Definition 1.3.1. (Polynomial system support) The support of a polynomial f_i is the set of its exponent vectors corresponding to nonzero coefficients.

For any subset $J \subset \{0, \dots, n\}$, let $r(J)$ denote the rank of the affine lattice generated by $\sum_{j \in J} A_j$. We assume that, for $I = \{0, \dots, n\}$, $r(I) = |I| - 1$, and $r(J) \geq |J|$ for any proper subset $J \subset I$.

Definition 1.3.2. (Newton polytope) Given a polynomial f_i its Newton polytope $N(f_i)$ is the convex hull of its support (fig. 1.6).

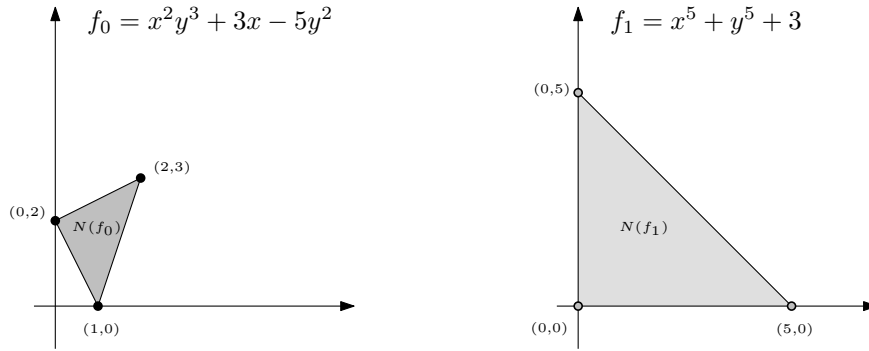


Fig. 1.6: The Newton polytopes of two polynomials.

Note that in contrast with the exponents of f its coefficients are not fixed.

Definition 1.3.3. (Sparse Resultant) The (sparse) Resultant R of f is a polynomial on the coefficients of f such that $R = 0$ iff f has a solution in $(\mathbb{C}^*)^n$.

This generalizes the determinant of an overconstrained linear system and the Sylvester resultant of two univariate polynomials. We call $N(R)$ the *Resultant polytope* and *extreme term* of R a monomial which corresponds to a vertex of $N(R)$. The following theorem describes how to compute an extreme term of R from a mixed subdivision of A .

Proposition 1.3.4. [Stu94, theorem 2.1] *Following the above notation and assumptions, given a system f and a mixed subdivision of the Minkowski sum of its supports, we get an extreme term of the resultant R equal to*

$$\pm \prod_{i=0}^n \prod_{\sigma} c_{iF_i}^{vol(\sigma)}$$

where $\sigma = F_0 + \dots + F_n$ is an i -mixed cell and $vol(\cdot)$ denotes Euclidean volume.

Example 1.3.5. As an illustration of the previous proposition consider the second mixed subdivision of fig. 1.4. Each i -mixed (for all $i \in \{0, 1, 2\}$) cell produce a sum of volumes according to prop. 1.3.4. For example, the 2-mixed cell $[(1, 0), (0, 2)] + [(0, 0), (0, 1)] + (0, 1)$ produce the monomial c_{12} of the Resultant extreme term. If we compute the monomials for all i -mixed cells then we get the extreme term $c_{00}c_{02}c_{11}^2c_{12}^4$ which corresponds to the point $(1, 0, 1, 0, 2, 0, 0, 4)$ in $(\sum_{i=0}^2 \#A_i)$ -dimensional space. Note that the third mixed subdivision of fig. 1.4 produce the same extreme term.

1.4 Enumeration algorithms

The above theory provides us with an algorithm that computes $N(R)$ given a polynomial system f . First we compute the supports A_0, \dots, A_n of f and by Cayley trick we get $\mathcal{C}(A_0, \dots, A_n)$. By enumerating all vertices of the secondary polytope $\Sigma(\mathcal{C}(A_0, \dots, A_n))$ we get all mixed subdivisions of $\bar{A} = A_0 + \dots + A_n$. Each of these subdivisions produces an extreme term of $N(R)$ by applying proposition 1.3.4.

Until now we have treated the enumeration of all vertices of the secondary polytope of a given points set as a black box. In this section we are going to study this problem and focus on two main approaches of enumerating regular triangulations. Briefly, the first one uses matroid theory and the second one the reverse search technique.

Problem. Enumerate all or some (with respect to a given property) triangulations of a given point set $A = a_1, a_2, \dots, a_m$ in \mathbb{R}^d .

If we want to enumerate all the triangulations, even in the planar case the complexity of this problem is unknown, though conjectured to be $\#\mathbf{P}$ -complete [Vaz04]. However, in the special case where the planar point set is in convex position (i.e. a convex m -gon) the number of all triangulations is the $m - 2$ nd Catalan number:

$$C_{m-2} = \frac{1}{m-1} \binom{2m-4}{m-2}$$

Regarding regular triangulations, the complexity of the corresponding enumeration problem is also unknown. Although, the number of these triangulations can be exponential in $|A|$. Thus, we focus on output-sensitive algorithms.

1.4.1 TOPCOM: Combinatorics of triangulations

The main goal here is to combinatorially characterize structures and properties such as polyhedral subdivisions and triangulations. This concept is illustrated in [PR03] and implemented in software package TOPCOM (*Triangulations of Points Configurations and Oriented Matroids*) [Ram02].

The basic idea of TOPCOM briefly goes as follows. Given a point set A in \mathbb{R}^d it first computes the main combinatorial structure named *chirotope*, computing only determinants in dimension d . After computing the chirotope, the algorithm can perform a number of computations purely combinatorially, that is without accessing the coordinates of points in A . These are, construct a triangulation from a point set, check if a triangulation is valid, perform a bistellar flip, compute a connecting component of a flip graph and compute all triangulations of A .

To explain this in further detail, we give now some basic definitions from matroid theory.

Definition 1.4.1. (signatures) A *signature* on a finite set S is a partition of S into three subsets, V_- , V_0 and V_+ . A signature is called positive if V_- is empty, and negative if V_+ is empty. Given a signature V_- , V_0 and V_+ on S , the set $V = V_- \cup V_+$ is called its support.

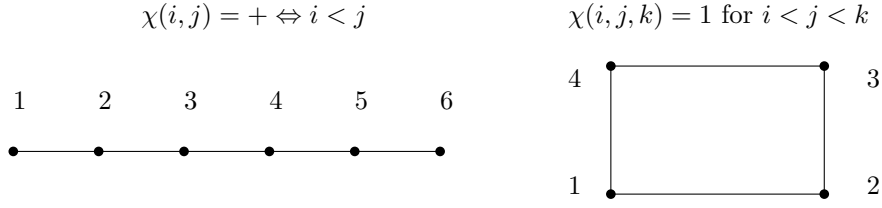


Fig. 1.7: Chirotopes in 1 and 2 dimensions.

Definition 1.4.2. (chirotope) The *chirotope* of a point set A in \mathbb{R}^d is the map

$$\chi : \begin{cases} [m]^{d+1} & \rightarrow \{+, 0, -\} \\ (i_1, i_2, \dots, i_{d+1}) & \mapsto \text{sign } \det(a_1, a_2, \dots, a_{d+1}) \end{cases}$$

Definition 1.4.3. (cocircuit) Let $\bar{C} \subseteq A$ spans a $d - 1$ -dim hyperplane in \mathbb{R}^d then a *cocircuit signature* on C is:

$$C : \begin{cases} [m] & \rightarrow \{+, 0, -\} \\ i & \mapsto \chi(\bar{C}, i) \end{cases}$$

with $C_+ = \{i \in [m] : C(i) = +\}$, $C_- = \{i \in [m] : C(i) = -\}$

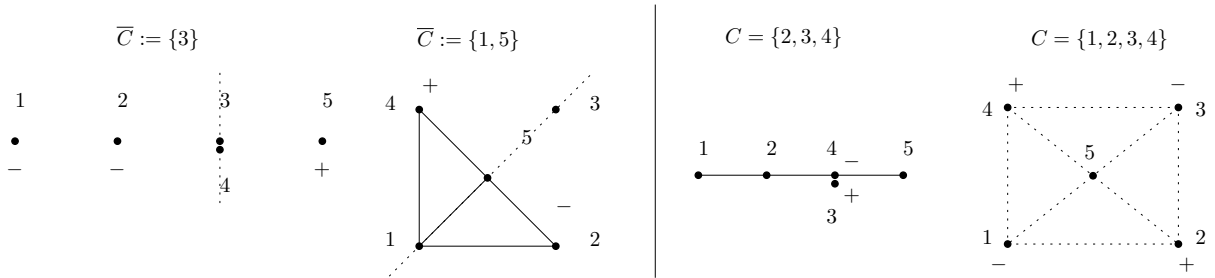


Fig. 1.8: Computing cocircuits [left] and circuits [right] using chirotopes.

Definition 1.4.4. (circuit signature) A *circuit signature* on Z , a set of $d + 2$ points in A is

$$Z : \begin{cases} [m] & \rightarrow \{+, 0, -\} \\ i_j & \mapsto (-1)^j \chi(C \setminus i_j) \\ i & \mapsto 0 \text{ if } i \notin C \end{cases}$$

We present now a combinatorial version of the properties in definition 1.1.1.

Proposition 1.4.5. ([PR03], proper intersection of simplices) *Two simplices of a pointset A in \mathbb{R}^d violate intersection property (IP) of polyhedral subdivision if and only if there is a circuit (Z_-, Z_+) of A with $Z_+ \subseteq \sigma$, $Z_- \subseteq \sigma$.*

Fig. 1.9: [left] Improper intersection detected by a circuit, [right] Interior facet covered by only one simplex.

Remark 1.4.6. A subset of A is a facet of A if and only if it is the zero set of a cocircuit having no positive elements, or if it is the zero set of a cocircuit having no negative elements.

Proposition 1.4.7. ([PR03], proper covering by simplices) *A partial triangulation T of a pointset A in \mathbb{R}^d violates union property (UP) of polyhedral subdivision if there is an interior facet of T lying in only one simplex of T .*

To check if a given triangulation is valid, first of all we can construct the set of all circuits. Since there are at most $\binom{m}{d+2}$ affinely dependent point sets in A , the possible circuits are that many. Similarly, we can construct the set of all cocircuits. Note that there are at most $\binom{m}{d}$ hyperplanes spanned by subsets of A . Thus the possible cocircuits are that many. The intersection and union properties can be checked by applying the combinatorial test of prop. 1.4.5, 1.4.7 to the set of all circuits and cocircuits respectively.

We now know how to check if a triangulation is valid using chirotopes. As mentioned before, the chirotope can be used to construct some triangulation and to flip between triangulations [PR03]. Providing that, one can finally formulate an enumeration algorithm of all regular triangulations.

Given a point set A in \mathbb{R}^d first of all the algorithm compute the chirotope. Then it constructs an initial regular triangulation. Starting from this it performs a Breadth First Search (BFS) in the graph of flips. It uses bistellar flips to go from one triangulation (vertex of the graph) to another. At each step the algorithm checks for regularity because a bistellar flip on a regular triangulation may produce a non regular triangulation. All the above computations are operated using the chirotope, except regularity test which is performed solving a linear program [Ram02]. Eventually, the algorithm enumerates all regular triangulations of A .

1.4.2 Enumeration of regular triangulations by reverse search

In this section we will present an output-sensitive enumeration algorithm of regular triangulations developed in [Mas95] and extended in [MII96]. This algorithm uses the reverse search technique [AF92] to traverse the graph of flips for a given point set. By using reverse search the algorithm uses space asymptotically equivalent to the space needed to store one triangulation. It is also discussed how the algorithm builds an initial triangulation and how it performs a regularity test on a triangulation.

For simplicity we assume general case position but the results can be extended to degenerate cases [IMTI02].

Data structures. Let A be a point set in \mathbb{R}^d , T a regular triangulation and T_R the number of all regular triangulations. We will first present the data structures used by the algorithm. A simplex of a triangulation is represented as a set of $d + 1$ points. A facet f can be seen as the intersection of two adjacent $d + 1$ -dimensional simplices s, s' and is

represented by the two points belong to s, s' but not in f . Denote $s = O(m^{\lfloor d/2 \rfloor})$ (prop. 1.1.15) the maximum number of simplices in T (i.e. the number of faces of $\text{conv}(A)$). Because each simplex must cover at least one facet of $\text{conv}(A)$ the number of facets of T is $O(ds)$. A triangulation is represented as a incidence graph with the simplices as vertices and their common facets as edges. This graph requires $O(ds)$ space.

The algorithm must also maintain all circuits of A satisfying link condition (def. 1.1.10). Every circuit represented by a $d+2$ set sorted in increasing order of point indices. All such circuits are maintained in a list in lexicographic order. The convex hull of a circuit consists of at most $d+1$ simplices so we represent it implicitly by this simplices. The number of simplices is $O(ds)$ and the list of circuits requires $O(ds)$ space.

At last, the algorithm maintains for each regular triangulation its volume vector.

Flips. When a flip is performed the above data structures has to be updated. For simplices in $O(ds)$ time we update the sorted list of simplices. For circuits, at most d^2 circuits are deleted and inserted in the list. Two circuits are compared with respect to lexicographic ordering in $O(d)$ time. The link condition can be checked in $O(d^2)$. Thus, the list of circuits can be updated in $O(d^2s)$ time. Finally, the volume vector can be updated in $O(d^4)$ time.

Regularity test and initial triangulation construction. Whether a triangulation is regular can be checked by solving a linear programming problem with ds strict inequality constraints in $m-d-1$ variables. This time is denoted by $LP(m-d-1, ds)$.

The construction of an initial regular triangulation can be done by constructing the Delaunay triangulation using a convex hull algorithm [AF92, Cha91, GKS90]. Alternatively, the triangulation with maximum volume vector among all triangulations can be used. This triangulation can be constructed from any triangulation by flipping to triangulations with lexicographically larger volume vectors.

Reverse search. The reverse search algorithm [AF92] enumerates a graph $G = (V, E)$ using constant space providing that there is an adjacency relationship between the vertices of the graph defining the edges and a father-child relationship in the graph. The algorithm constructs a spanning tree in G like Breadth First Search (BFS) or Depth First Search (DFS) algorithms using the adjacency relationship. A father-child relationship f is used to reduce the space complexity. This relationship can be seen as an optimization function on the vertices of G . Therefore f defines a directed rooted spanning tree R on G . The reverse search algorithm traverses R in a depth-first manner without keeping the search path in memory because being on a vertex v the algorithm knows the parent of v in R and the children of v not visited yet. To perform the latter we need an arrangement of the children for each vertex.

The reverse search algorithm for the secondary polytope uses as adjacency relationship the flips and as father-child relationship the lexicographic maximization of volume vectors. Additionally, the algorithm needs an arrangement of the children for each vertex. From a vertex on R each child performed by flipping with respect to some circuit. The data structure maintenance of all circuits in lexicographic order provide us with the desirable

arrangement.

Proposition 1.4.8. ([MII96], theorem 4) *Regular triangulations of m points in \mathbb{R}^d in general position can be enumerated in $O(dsLP(m-d-1, ds)T_R)$ time and $O(ds)$ working space.*

Proposition 1.4.9. ([IMTI02], theorem 13) *Regular triangulations of m points in \mathbb{R}^d can be enumerated in $O(d^2s^2LP(m-d-1, s)T_R)$ time and $O(ds)$ working space.*

1.4.3 Implementation issues

Although, these algorithms solve the problem of enumeration of regular triangulations their complexities are prohibitive for applications we are interested in such as implicitization (see chapter 3). In experimental analysis presented in [Fis09] TOPCOM seems faster than the reverse search approach but it uses much more memory.

The reverse search algorithm has constant memory consumption but its running time is prohibitive if the number of regular triangulations is large. For example, the algorithm halts with input $A = \{(0, 0), (2, 0), (4, 0), (6, 0), (8, 0), (0, 1), (1, 1), (2, 1), (3, 1), (4, 1), (5, 1), (6, 1), (7, 1), (8, 1)\}$ and $A' = \{(0, 0, 0, 0), (0, 2, 0, 0), (2, 0, 0, 0), (2, 2, 0, 0), (0, 0, 0, 1), (0, 2, 0, 1), (2, 0, 0, 1), (1, 2, 0, 1), (2, 2, 0, 1), (0, 1, 1, 0), (0, 2, 1, 0)\}$ which has 42168 and 76280 regular triangulations respectively [Fis09].

Even TOPCOM halts for some datasets (for an example of 15 4-dimensional points see twisted sphere in [Fis09]). In addition to that if we naively store the computed triangulations we need half gigabyte for 800000 triangulations. These large numbers of triangulations often occur when we apply implicitization on surfaces [EK03, Fis09].

It follows that the number of vertices of a Secondary polytope can be exponential in $|\overline{A}|$. On the other hand, by proposition 1.3.4 there is a many to one correspondence of secondary vertices to the vertices of the Resultant polytope, illustrated by the experiments in [Fis09]. For the Resultant polytope, we only know a weak exponential upper bound on the number of vertices [Stu94, prop.6.1]. Thus, if we only want to compute $N(R)$ we focus on algorithms that enumerate the smallest possible subset of secondary vertices sufficient to compute $N(R)$. The next chapter presents theory and results that may help towards this direction.

CHAPTER 2

Mixed cell configurations and R-equivalent classes

In the previous chapter we show how to compute the Resultant polytope using enumeration algorithms of all regular triangulations. Our goal here is to study the complexity of this method and finally to optimize it. The first section is about equivalent classes of mixed subdivisions and Ξ polytopes. In the second section we study flips that connect two subdivisions that correspond to different extreme terms of $N(R)$. Finally, we present a case study on the number of vertices of the Secondary and Resultant polytopes and the number of i -mixed cell configurations. The results of this section are also published in [EFK10].

2.1 Mixed cell configurations

Let A_0, A_1, \dots, A_n be point sets in \mathbb{R}^d and $\bar{A} = A_0 + A_1 + \dots + A_n$ be their Minkowski sum. By definition 1.2.2, a Minkowski cell c can be written as a Minkowski sum $F_0 + \dots + F_n$ for certain subsets $F_0 \subseteq A_0, \dots, F_n \subseteq A_n$. Equivalently, c can be represented as the set $\{F_0, F_1, \dots, F_n\}$.

Definition 2.1.1. (Minkowski cell type) Let S be a mixed subdivision and $c \in S$ a Minkowski cell. Then the type of the cell c is the set $\tau(c) = \{i \in \{0, \dots, n\} : |F_i| > 1\}$.

Definition 2.1.2. (I -mixed cell configuration) A cell $c = \{F_0, F_1, \dots, F_n\}$ is called I -mixed if $I = \tau(c)$. An I -mixed cell configuration is the set

$$S^I := \{(F_i \mid i \in I) \mid c \in S \text{ and } \tau(c) = I\}$$

where S is a given mixed subdivision.

Note that S^I is not the mixed subdivision of $A_i, i \in I$ because S^I is not necessarily convex (see $\Xi(A_0, A_2)$ in figure 2.2 for a counterexample).

The i -mixed cells, which are also fine, prescribed in definition 1.2.2 for the case $n = d$ are I -mixed cells where $I = \{0, 1, \dots, n\} - \{i\}$.

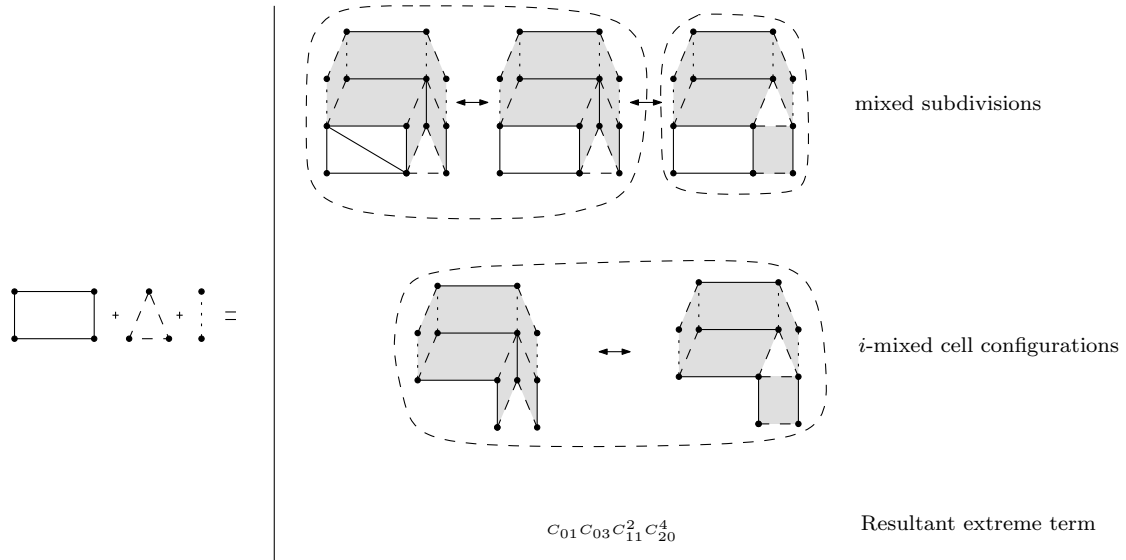


Fig. 2.1: The classification of i -mixed configurations on mixed subdivisions and the R-equivalent classification on i -mixed configurations.

If $I = \{0, 1, \dots, n\}$ we call the I -mixed cell *full-mixed* cell and the I -mixed cell configuration, *full-mixed* cell configuration.

If $n = d - 1$, the full-mixed cell configurations are the equivalence classes among all mixed subdivisions, where two such subdivisions are equivalent if and only if they share the same mixed cells as defined in [MV97].

If $n = d$, there are no full-mixed cells, that is cells c with $\tau(c) = \{0, 1, \dots, n\}$. However, we can have sets of cells c^* such that $\tau(c^*) = \{0, 1, \dots, n\}$. We will see in the next section that these kind of sets of cells are very interesting (see 2.2.1).

When $n = d$, we focus on the i -mixed cells in order to compute the vertices of $N(R)$. In [Kon06], there is an extension of mixed cells configurations of [MV97] to classes containing the same i -mixed cells for all $i \in \{0, \dots, n\}$, called i -mixed cell configurations. It turns out that these configurations are not I -mixed cell configurations for any $I \subseteq \{0, 1, \dots, n\}$.

We now characterize the flips between i -mixed cell configurations, and generalize the flip defined in [MV97] between mixed cell configurations.

We shall say that a circuit Z of a triangulation T supported on Z , involves an i -mixed cell $F_0 + \dots + F_n$, if the cell $\mathcal{C}(F_0, \dots, F_n)$ of T does not belong to the triangulation obtained by flipping on Z .

Proposition 2.1.3. ([Kon06, proposition 4.3.2]) *Let $Z = (Z_0, \dots, Z_n)$ be a circuit and T a triangulation supported on Z . Suppose that Z involves an i -mixed cell $F_0 + \dots + F_n$. Then, there exists $r \in \{0, \dots, n\}$, and $c \in A_r$ s.t. for all $i \neq r$, $Z_i = F_i$ or $Z_i = \emptyset$, and $Z_r = F_r \cup \{c\}$ or $Z_r = \{v_r, c\}$, where v_r is a vertex of edge F_r .*

A flip on a circuit as described in this theorem destroys at least one i -mixed cell leading to a new i -mixed cell configuration. Moreover, we can check efficiently if a circuit satis-

fies the conditions of prop. 2.1.3 by examining only the cardinalities of the sets Z_i . An algorithm using these flips enumerates only the i -mixed cell configurations, without enumerating all mixed subdivisions, which are more numerous. On the other hand, i -mixed cell configurations are more numerous than the vertices of $N(R)$ because there is a many to one relationship between these configurations and vertices of $N(R)$ (see fig. 2.1). The previous discussion give rise to the following result.

Remark 2.1.4. Given A_0, A_1, \dots, A_n points sets in \mathbb{R}^d with Minkowski sum $\bar{A} = A_0 + A_1 + \dots + A_n$, the number of mixed subdivisions of \bar{A} are more than or equal to the number of their i -mixed cell configurations which is more than or equal to the number of Resultant extreme terms.

For an illustration of this remark see figures 2.2, 2.1 and example 2.1.12.

2.1.1 Ξ polytopes

The Ξ *polytope* is defined in [MC00] for $n \leq d - 1$. We will present Ξ polytopes and we prove that the special case of Ξ polytope when $n = d$ is the Resultant polytope. Let $m = \sum_{i=0}^n |A_i|$.

If we translate the GKZ-vector of definition 1.1.4 using mixed subdivisions we get the following characteristic vector for mixed subdivisions.

Remark 2.1.5. Let S be a mixed subdivision and $c \in S$ a Minkowski cell.

Definition 2.1.6. (mixed GKZ-vector) Let S be a mixed subdivision of \bar{A} . Then the mixed GKZ-vector is $\Phi_S(\bar{A}) = (\phi_{S,1}(\bar{A}), \dots, \phi_{S,m}(\bar{A}))$ where

$$\phi_{S,j}(\bar{A}) = \sum_{c \in S: a_j \in F_i} \text{vol}(\mathcal{C}(c))$$

In other words, $\phi_{S,j}$ expresses for point $a_j \in \bigcup_i = 0^n A_i$ the sum of the volumes of all simplices in the corresponding (with respect to Cayley trick) triangulation T whose i -th summand includes a_j . Essentially, $\Phi_S(\bar{A})$ is the same as $\Phi_T(\bar{A})$ of definition 1.1.4 for the corresponding triangulation T of the mixed subdivision S . If we restrict the sum of the volumes to simplices with certain properties we get the following vectors.

Definition 2.1.7. (I -mixed GKZ-vector) Let S be a mixed subdivision of \bar{A} and $I \subseteq \{0, 1, \dots, n\}$. Then the I -mixed GKZ-vector is $\Phi_S^I(\bar{A}) = (\phi_{S,1}^I(\bar{A}), \dots, \phi_{S,m}^I(\bar{A}))$ where

$$\phi_{S,j}^I(\bar{A}) = \sum_{c \in S: \tau(c) \cup \{i\} = I, a_j \in F_i} \text{vol}(\mathcal{C}(c))$$

$c = \sum_o^n F_i$ and a_j ranges over $\bigcup_i = 0^n A_i$.

Definition 2.1.8. (mixed secondary polytope) The mixed secondary polytope Ξ of pointsets A_0, A_1, \dots, A_n in \mathbb{R}^d is

$$\Xi(A_0, A_1, \dots, A_n) := \text{conv} \left(\Phi_S^{\{0,1,\dots,n\}}(\bar{A}) \mid S \text{ is a mixed subdivision of } (A_0, A_1, \dots, A_n) \right)$$

The following proposition shows that these Ξ polytopes compose the Secondary polytope.

Proposition 2.1.9. ([MC00, theorem 4.6]) *The Secondary polytope of \bar{A} can be decomposed in mixed secondary polytopes*

$$\Sigma(\bar{A}) = \sum_{I \subseteq \{0,1,\dots,n\}} \Xi(A_i | i \in I)$$

where the sum denotes the Minkowski sum and the summands are embedded in the same $(\sum_{i=0}^n |A_i|)$ -dimensional space. Additionally, I ranges over all subsets of $\{0, 1, \dots, n\}$.

For the case $n = d$ the following result can be obtained if we observe that definition 2.1.7 when $I = \{0, 1, \dots, n\}$ and proposition 1.3.4 yield the same vectors $\Phi_S^I(\bar{A})$ given the same mixed subdivision S .

Proposition 2.1.10. *If $n = d$ then $\Xi(A_0, A_1, \dots, A_n) = N(R)$.*

Proof. Let S a mixed subdivision of \bar{A} and $I = \{0, 1, \dots, n\}$. Also recall the construction of an extreme term of $N(R)$ given a mixed subdivision as defined in proposition 1.3.4. $\Phi_S(\bar{A})$ by definition 2.1.7 has as i -coordinate the sum of volumes of simplices that contain a_i . This is the way Secondary polytopes are constructed. Ξ polytopes use $\Phi_S^I(\bar{A})$ instead. $\Phi_S^I(\bar{A})$ by definition 2.1.6 has as i -coordinate the sum of volumes of simplices that contain $a_i \in A_j$ and their corresponding Minowski cell is j -mixed. Equivalently, every j -mixed cell $F_0 + \dots + F_{j-1} + a_i + F_{j+1} \dots + F_n$ contributes its volume to the i -coordinate of $\Phi_S^I(\bar{A})$. That is, if a_i is the ℓ -th point in A_j then this volume can be seen as the exponent of the $c_{\ell j}$ symbolic variable of the extreme term constructed by S as defined in proposition 1.3.4. Thus, $\Phi_S^I(\bar{A})$ when $I = \{0, 1, \dots, n\}$ yields an extreme term of $N(R)$ as the formula of proposition 1.3.4 given a mixed subdivision S of \bar{A} . So $\text{conv}(\Phi_S^I(\bar{A}))$ for all mixed subdivisions S is equal to $N(R)$ and by definition 2.1.8 it is also equal to $\Xi(A_0, A_1, \dots, A_n)$. \square

From [Stu94, corollary 5.1] we know that $N(R)$ is a summand of Secondary polytope. Here, propositions 2.1.9 and 2.1.10 lead to the same result. In addition to that, we now know a way to compute the other summands of the Secondary polytope.

Corollary 2.1.11. $\Sigma(A) = \sum_{I \subseteq \{0,1,\dots,n\}} \Xi(A_i | i \in I) + N(R)$

Example 2.1.12. Let $A_0 = \{(0, 0), (1, 0), (0, 1), (1, 1)\}$, $A_1 = \{(0, 0), (1, 0)\}$, $A_2 = \{(1, 0), (0, 1)\}$. The Secondary polytope of $\mathcal{C}(A_0, A_1, A_2)$ with mixed subdivisions of \bar{A} as vertices is depicted in figure 2.2. The i -mixed cell configurations are the dotted classes and the Resultant extreme terms the dashed classes. The Ξ polytopes are also depicted in this figure. The vertices of Ξ polytopes where $I = \subseteq \{0, 1, 2\}$ correspond to mixed cell configurations $S^{\{0\}}, S^{\{1\}}, S^{\{2\}}, S^{\{0,1\}}, S^{\{1,2\}}, S^{\{0,2\}}$ and depicted by drawing them as $\sum_{i \in I} F_i$. Observe that the $\Xi(A_0, A_1, A_2)$ polytope is the same as $N(R)$. The vertices of this polytope correspond to sets of cells.

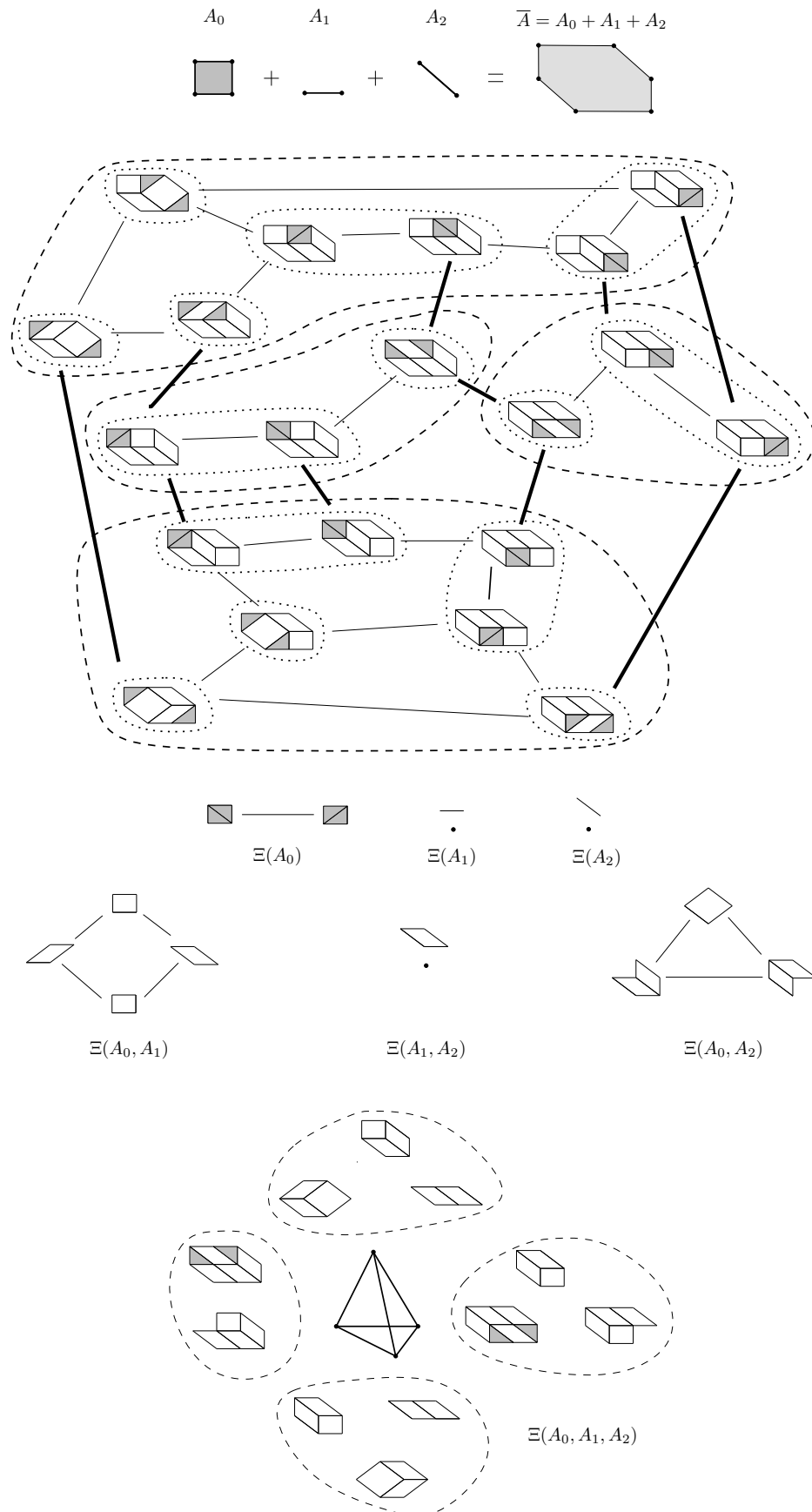


Fig. 2.2: An illustration of example 2.1.12.

2.2 R-equivalent classes

By prop. 1.3.4, several mixed subdivisions may produce the same extreme term of the Resultant. We call these subdivisions *R-equivalent*. Similarly, two subdivisions may lead to the same extreme term, even if they belong to the same *i*-mixed cell configuration (see fig. 2.1). These R-equivalent classes correspond to the vertices of $N(R)$. There are some flips that connect two subdivisions in different R-equivalent classes, hence they correspond to the edges of $N(R)$.

Sturmfels [Stu94, thm.5.2] calls these flips *cubical*. Consider the union of cells affected by one such flip. If the union, lifted generically to \mathbb{R}^{d+1} , forms an affine cube, i.e. equals the Minkowski sum of $n + 1$ edges, then the flip is cubical and consists in replacing the “bottom” subdivision by the “top” subdivision, or vice versa (fig. 2.3, fig. 2.4). However, this definition of cubical flips is not algorithmically efficient, so we provide a more algorithmic characterization.

Let us start with the generic case, where every two faces of the same dimension in two different $\text{conv}(A_i)$ are not parallel.

Lemma 2.2.1. *Let S be a mixed subdivision of $A_0 + \dots + A_n$. Then S has a cubical flip iff there exists a set $\{C_0, \dots, C_n\}$ of *i*-mixed cells $C_i = F_0 + \dots + a_i + \dots + F_n$, for $i = \{0, 1, \dots, n\}$, where $a_i \in F_i \subseteq A_i, |F_i| = 2$, such that, if $C = \bigcup_{i=0}^n C_i$, then $C = F_0 + \dots + F_n$. We say S is supported on C . The cubical flip on S consists of substituting, in every C_i , point a_i with $F_i - \{a_i\}$.*

If the generic position assumption does not hold, lem. 2.2.1 does not hold, so we generalize this characterization using triangulations. Recall that the set C of *i*-mixed cells corresponds by Cayley trick to a set Z of simplices and a flip between two mixed subdivisions is a flip between the two corresponding triangulations. Generically, C has $n + 1$ cells and Z has $n + 1$ simplices. The union of these simplices contains $2n + 2$ points in a space of dimension $n + d$. If $d = n$, this union of simplices is a circuit. In degenerate cases, there may exist lower dimensional circuits and C may have $< n + 1$ cells. As an illustration compare the generic example (fig. 2.3), where C has 3 cells, with the degenerate example (fig. 2.4), where C has only 2 cells.

Theorem 2.2.2. *Let S be a mixed subdivision of $A_0 + \dots + A_n$, and T the corresponding triangulation with respect to Cayley’s trick. Then S has a cubical flip if there exists a set $C = \bigcup_{i=0}^k C_i \subseteq S$ of *i*-mixed cells, as in lem. 2.2.1 and, additionally, the corresponding set Z of simplices in T supports a bistellar flip. The cubical flip on S is the bistellar flip of T supported on Z .*

The mapping of cubical flips edges of $N(R)$ is many to one. When a cubical flip is supported on set C , we say that the edge is of type C . Many cubical flips may be supported on the same set C . The types of all Resultant edges can be easily enumerated: they are all possible Resultant polytopes of subsets of A_i ’s with cardinality two. This enumeration also yields the corresponding edge direction, i.e. the difference vector between the two endpoints

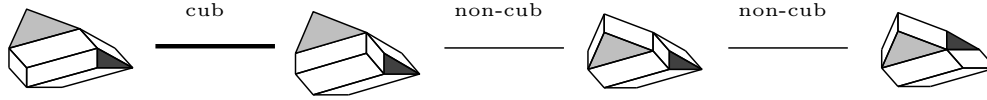


Fig. 2.3: An example of a cubical and two non cubical flips.

of $N(R)$. More generally, all faces of $N(R)$ are Minkowski sums of Resultant polytopes corresponding to subsystems of A_0, \dots, A_n . Conversely, every resultant polytope defined on subsets of the A_i 's appears on a suitable face of $N(R)$ [Stu94].

The previous theorem is an algorithmic test which can be used for the enumeration of $N(R)$. Unfortunately, this is not possible. Let the graph $G = (V, E)$ where V contains the vertices of the secondary polytope which are adjacent to at least one cubical flip and E contains the edges that correspond to cubical flips.

Remark 2.2.3. G is not always connected.

To see this just consider the example 2.2.4 which is illustrated in figure 2.5.

Example 2.2.4. Let $A_0 = \{(0, 0), (1, 2), (4, 1)\}$, $A_1 = \{(0, 1), (1, 0)\}$, $A_2 = \{(0, 0), (0, 1), (2, 0)\}$, which satisfy the general position assumption. The Secondary polytope of $\mathcal{C}(A_1, A_2, A_3)$ is depicted in fig. 2.5 (left). One can see the R-equivalent classes (dotted) as well as the cubical flips (bold) which connect these classes. All the other flips (non bold) are non-cubical flips. The Resultant polytope can be seen as the polytope with R-equivalent classes as vertices and cubical flips as edges. To each Resultant vertex corresponds one or more mixed subdivisions, and to each edge one or more cubical flips (9 flips to 11 edges). Here, the number of mixed subdivisions is the same as the number of i -mixed cell configurations i.e. 36. $N(R)$ has 6 vertices, and 11 edges corresponding to 9 different cubical flips (fig. 2.5 right) which are all generic.

2.2.1 Secondary, Resultant polytopes and i -mixed cell configurations

Let $\Sigma, \mathcal{M}, \mathcal{Res}$ denote the sets of vertices of the Secondary polytope of $\mathcal{C}(A_0, A_1, \dots, A_n)$, all i -mixed cell configurations of $\mathcal{C}(A_0, A_1, \dots, A_n)$ and vertices of the Resultant polytope respectively. Moreover, $|\Sigma|, |\mathcal{M}|, |\mathcal{Res}|$ denote the cardinalities of these sets. We offer a case study on these quantities, and focus on $d = n$.

When $d = n = 1$, every Minkowski cell is an edge, i.e., a sum of an edge and a vertex, thus an i -mixed cell. Then $|\Sigma| = |\mathcal{M}|$, and they are generally larger than $|\mathcal{Res}|$. $|\mathcal{Res}|$ is $\binom{m_0+m_1-2}{m_0-1}$ [GKZ90].

For arbitrary d, n , if all $|A_i| \leq 3$, then $|\Sigma| = |\mathcal{M}|$. To see this, recall that for any fine Minkowski cell $F = \sum_{i=1}^n F_i$, it holds that $\sum_{i=1}^n \dim(F_i) = d$. So, F is not i -mixed if and only if for some F_i , we have $\dim(F_i) > 1$. Since $|A_i| \leq 3$, by the pigeonhole principle, every non i -mixed cell is a sum of $n - 2$ edges, two vertices and a triangle. So the union of every pair of non i -mixed cells can be written uniquely.

The smallest case that this does not hold is when there exists i s.t. $|A_i| = 4$, and $|A_j| \leq 3, \forall j \neq i$.

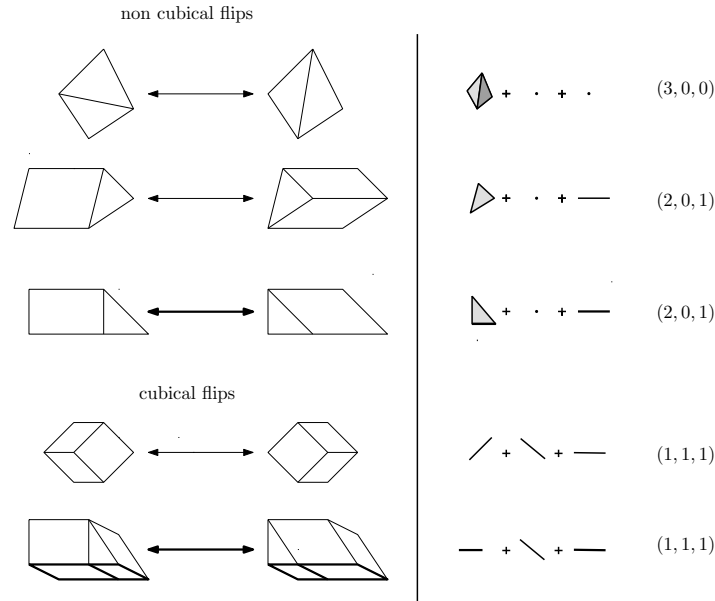


Fig. 2.4: Generic flips and degenerate (bold; two edges from different A_i 's are parallel) ones.

Example 2.2.5. An instance of the smallest case, for $d = n = 2$, is $A_0 = \{(0, 0), (0, 1), (2, 0), (2, 1)\}$, $A_1 = \{(0, 0), (1, 1), (2, 0)\}$, $A_2 = \{(0, 0), (0, 1)\}$, where $|\Sigma|$, $|\mathcal{M}|$, and $|\mathcal{R}es|$ are 122, 98, and 8 respectively. Another one is depicted in fig. 2.1.

For arbitrary d, n , if for all i , $|A_i| = 2$, then $|\Sigma| = |\mathcal{M}| = |\mathcal{R}es|$. This is the case where all flips are cubical, every Minkowski cell is a sum of edges, called zonotope, and the mixed subdivisions are zonotopal tilings. The above discussion proves the following.

Lemma 2.2.6. If $d = n = 1$, or for all i , $|A_i| \leq 3$, then $|\Sigma| = |\mathcal{M}|$ and they are at least as large as $|\mathcal{R}es|$. If for all i , $|A_i| = 2$, then $|\Sigma| = |\mathcal{M}| = |\mathcal{R}es|$.

In addition to the case analysis above, we study relevant experimental results presented in next chapter. For the nonce, we consider some (highly) nontrivial examples corresponding to the implicitization of a parametric sphere [EK05].

Example 2.2.7. The A_i 's are $\{(0, 0), (0, 2), (2, 0), (2, 2)\}$, $\{(0, 0), (1, 0), (0, 2), (2, 0), (1, 2), (2, 2)\}$, $\{(0, 0), (0, 1), (0, 2)\}$, and $|\Sigma|, |\mathcal{M}|$ and $|\mathcal{R}es|$ are 76280, 32076 and 95 respectively.

The A_i 's are $\{(0, 0), (1, 0), (0, 2), (2, 0), (1, 2), (1, 2)\}$, $\{(0, 0), (0, 2), (1, 1), (2, 0), (2, 2)\}$, $\{(0, 0), (2, 0)\}$ and $|\Sigma|, |\mathcal{M}|$ and $|\mathcal{R}es|$ are 104148, 43018 and 21 respectively.

Our ultimate goal is an algorithm to enumerate all vertices of $N(R)$ without enumerating the entire Σ or \mathcal{M} . At present, cubical flips do not suffice. In particular, if we consider only cubical flips the resulting graph is disconnected (see remark 2.2.3 and figure 2.5). To this end we need a unique representation of the resultant vertices and some kind of flip based on the cubical flip.

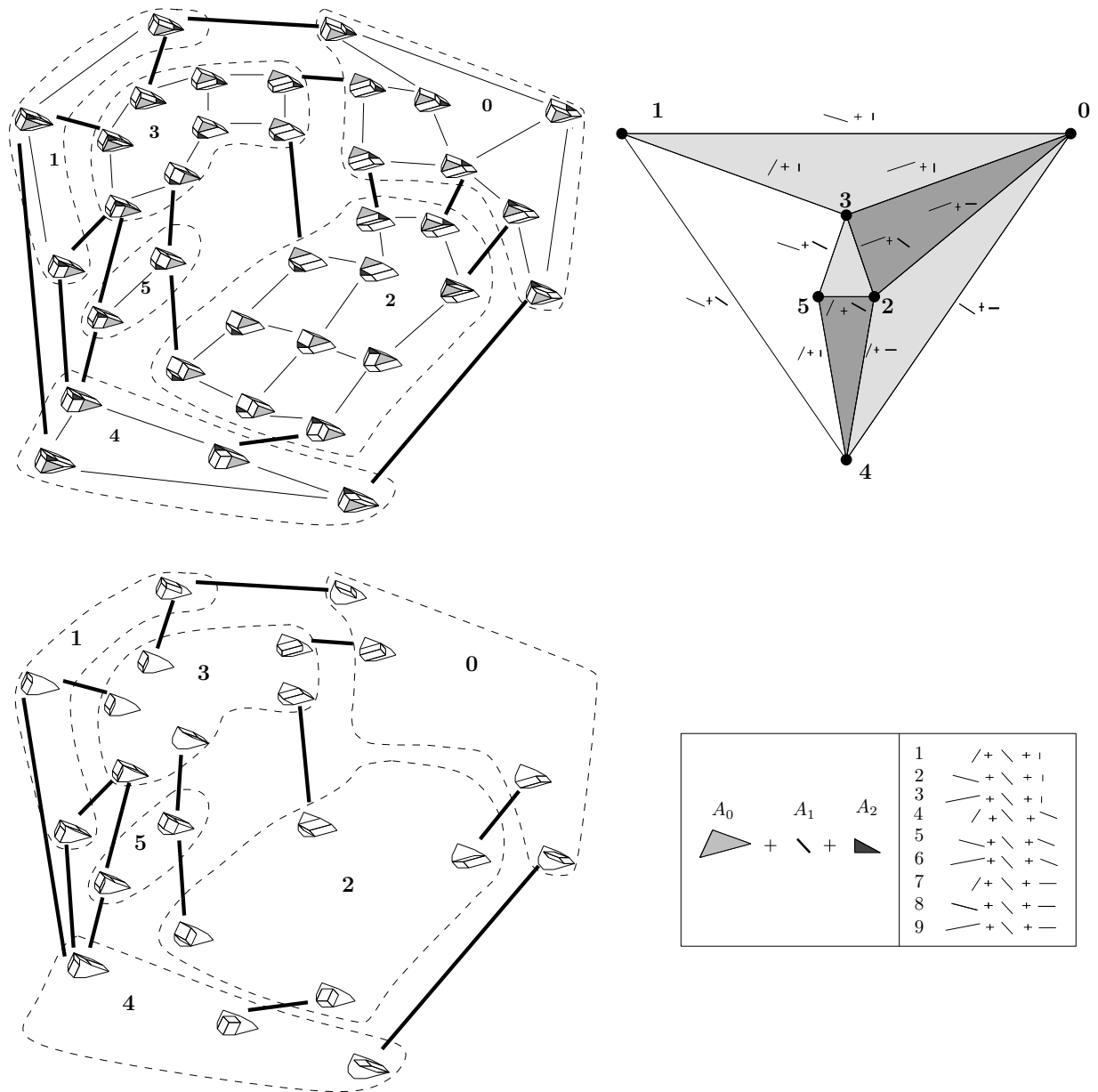


Fig. 2.5: An illustration of example 2.2.4. [up-left] The Secondary polytope with the R-equivalent classes (dotted) and the cubical flips (bold). [up-right] The Resultant polytope. [bottom-left] The Secondary polytope with the cubical flips only. The vertices are depicted by the convex hull of the mixed subdivision and the cells that take part on the flip. [bottom-left] The input point sets and the cubical flips.

CHAPTER 3

Experiments, applications and conclusions

In this chapter we present an application of the enumeration of $N(R)$ vertices to the problem of implicitization. Implicitization is an important elimination problem. In addition to that we present experimental results of an implicitization algorithm that uses as a basic part the enumeration of $N(R)$ vertices. The input of our experiments is some famous curves and surfaces. These results are also presented in [Fis09]. The chapter finishes with a conclusion and future work section.

3.1 Implicitization

We will present the implicitization algorithm IPSOS [EK03], which given a hypersurface in parametric form computes a super-set of the support set of the hypersurface's implicit equation.

Let

$$x_i = \frac{P_i(t)}{Q(t)}, i = \{0, 1, \dots, n\}$$

the parametric form of a hypersurface. Hence, $n = 1$ for curves and $n = 2$ for surfaces. Consider the polynomial system $f_i = x_i Q(t) - P_i(t) \in \mathbb{C}[t]$, $t = (t_0, t_1, \dots, t_n)$, with $A_i \subset \mathbb{Z}^n$. The polynomial system contains generic coefficients c_{ij} in the place of the original ones of $Q(t), P_i(t)$. If some constraints are satisfied (see, [EK03]) the implicit equation of the hypersurface is the Resultant of the system of polynomials f_i .

The IPSOS algorithm's steps are the following:

1. Construct $f_i = \sum c_{ij} t^{a_{ij}} \in \mathbb{C}[t]$ from the given parametric equations, where $a_{ij} \in A_i$ and c_{ij} generic coefficients.
2. Compute the $N(R)$ of the system of polynomials f_i

3. Compute the lattice (integer) points that lay inside $N(R)$. These form together with $(N(R)$ extreme terms a super-set of the support set of the hypersurface's implicit equation. This super-set form a polynomial R' .
4. Substitute x_i terms for c_{ij} coefficients in the monomials of R' .
5. Using bounds in the degree of the implicit equation eliminate the monomials that does not satisfy the criteria.

In the previous sections we have extensively discussed the step 2 of this algorithm, the algorithm that computes the Newton polytope of the Resultant. The third step is a problem of independent interest; see [LHTY04, TA97] for a discussion on algorithms and software that solve this problem. The last steps can be performed by algorithms using linear algebra. We will not focus on these problems; see [EK03] for more details.

3.2 Experiments - Software

A basic part of this thesis is the experimental analysis of the algorithms that compute $N(R)$ that may lead to new ideas for optimal algorithms. For this reason there have been developed a software package in Python. This package can be seen as an implementation of the IPSOS algorithm as well as a collection of software that implements algorithms for problems discussed in this thesis.

The input of the algorithm are some famous curves and surfaces from bibliography [Kok]. By applying step 1 of IPSOS algorithm above we can transform the parametric equations to a polynomial system and extract the supports A_0, A_1, \dots, A_n . The main purpose of these experiments is to combine quantities such as the size of the Secondary polytope of $mathcal{C}(A_0, A_1, \dots, A_n)$, the number of i -mixed cell configurations, the size of $N(R)$ and the number of lattice points inside $N(R)$. In addition to that, we want to compare the two methods of enumerating regular triangulations presented in section 1.4.2.

The symbolic computations are done using the python library `sympy` [Sym10]. Both TOPCOM [Ram02] and the algorithm from [MII96] are used to compute all regular triangulations of a point configuration. PORTA [TA97] is used to compute the lattice points inside the Resultant polytope. Finally, Polymake [GJ00] is used as visualization tool.

There have been a wiki page [Fis09] developed with the experimental results which are presented in the following two subsections. The goal of this wiki page is to present some implicitization methods on a collection of curves and surfaces. Additionally, it should focus on the comparison of the methods and software packages that implement the steps of the implicitization. For example a comparison between the running times of TOPCOM and the method of [MII96].

3.2.1 Experiments on curves

For the case of curves, there are two equations on one variable t . Also a, b, c are constants.

CURVES	# mixed subdivisions	# i -mixed cell configurations	# $N(R)$ vertices	# points in $N(R)$
astroid $a \cos(t)^3, a \sin(t)^3$	289	289	35	454
cardioid $a(2 \cos(t) - \cos(2t)), a(2 \sin(t) - \sin(2t))$	37	37	10	33
circle $\cos(t), \sin(t)$	5	5	3	4
conchoid $a + \cos(t), a \tan(t) + \sin(t)$	12	12	4	6
ellipse $a \cos(t), b \sin(t)$	5	5	3	4
folium of Descartes $3at/(1 + t^3), 3at^2/(1 + t^3)$	14	14	6	10
involute of a circle $a(\cos(t) + t(\sin(t))), a(\sin(t) - t \cos(t))$	14	14	6	7
nephroid $a(3 \cos(t) - \cos(3t)), a(3 \sin(t) - \sin(3t))$	289	289	35	454
Plateau curve $a \sin(3t)/\sin(t), 2a \sin(2t)$	94	94	15	55
Talbot's curve $(a^2 + c^2 \sin(t)^2) \cos(t)/a,$ $(a^2 - 2c^2 + c^2 \sin(t)^2) \sin(t)/b$	1944	1944	84	1600
tricuspid $a(2 \cos(t) + \cos(2t)), a(2 \sin(t) - \sin(2t))$	37	37	10	33
witch of Agnesi $at, a/(1 + t^2)$	2	2	2	2

3.2.2 Experiments on surfaces

For the case of surfaces, there are three equations on two variables t, s .

SURFACES	# mixed subdivisions	# i -mixed cell configurations	# $N(R)$ vertices	# points in $N(R)$
cylinder $\cos(t), \sin(t), s$	5	5	3	4
cone $s \cos(t), s \sin(t), s$	122	98	8	14
paraboloid $s \cos(t), s \sin(t), s^2$	122	98	8	37
surface of revolution $s \cos(t), s \sin(t), \cos(s)$	122	98	8	37
sphere $\sin(t) \cos(s), \sin(t) \sin(s), \cos(t)$	104148	43018	21	186
sphere2 $\cos(t) \cos(s), \sin(t) \cos(s), \sin(s)$	76280	32076	95	776
stereographic sphere $2t/(1+t^2+s^2), 2s/(1+t^2+s^2),$ $(t^2+s^2-1)/(1+t^2+s^2)$	3540	3126	22	283
twisted sphere $3 \cos(s) \cos(t), 3 \cos(s) \sin(t), 3 \sin(s) - 2t$	> 1812221	-	-	-

3.3 An example: the equation of circle

As an illustration of all the above we give an example of the implicitization of the parametric equations of the circle. Given the circle in parametric form:

$$\begin{cases} x = \cos(t) \\ y = \sin(t) \end{cases}$$

we obtain:

$$\begin{cases} x = \frac{-t^2+1}{s} \Rightarrow -t^2 + sx - 1 = 0 \\ y = \frac{2t}{s} \Rightarrow 2t - sy = 0 \\ z = t^2 - s + 1 \end{cases}$$

by substituting $\cos(t), \sin(t)$ with $\frac{-t^2+1}{t^2+1}, \frac{2t}{t^2+1}$ and setting $s = t^2 + 1$. Therefore we get 3 systems in 2 variables instead of 2 in 1 variable.

By renaming the constant terms with respect to variables t, s with symbolic terms we have the following system:

$$\begin{cases} C_{02}t^2 + C_{01}s + C_{00} \\ C_{11}t + C_{10}s \\ C_{22}t^2 + C_{21}s + C_{20} \end{cases}$$

So, the resulting supports are:

$$\begin{cases} \{\{0, 0\}, \{0, 1\}, \{2, 0\}\} \\ \{\{0, 1\}, \{1, 0\}\} \\ \{\{0, 0\}, \{0, 1\}, \{2, 0\}\} \end{cases}$$

the convex hulls of these sets are the points of the Newton polytopes.

Applying the Cayley trick we have the following set of points:

$$CA = \{\mathbf{0}:\{0, 0, 0, 0, 1\}, \mathbf{1}:\{0, 1, 0, 0, 1\}, \mathbf{2}:\{2, 0, 0, 0, 1\}, \mathbf{3}:\{0, 1, 0, 1, 1\}, \\ \mathbf{4}:\{1, 0, 0, 1, 1\}, \mathbf{5}:\{0, 0, 1, 0, 1\}, \mathbf{6}:\{0, 1, 1, 0, 1\}, \mathbf{7}:\{2, 0, 1, 0, 1\}\}$$

This point set has 26 regular triangulations. The first one is:

$$\{\{0, 1, 2, 3, 5\}, \{0, 2, 3, 4, 5\}, \{1, 2, 3, 5, 6\}, \{2, 3, 4, 5, 6\}, \{2, 3, 4, 6, 7\}, \{2, 4, 5, 6, 7\}\}$$

For each one of these we can compute its GKZ vector. For example the GKZ vector of the first triangulation above is

$$\{4, 4, 10, 8, 6, 9, 6, 3\}$$

The convex hull of this vectors is the Secondary polytope.

Applying a reverse procedure from that of the Cayley trick we can take 26 mixed subdivisions, each one corresponds to one regular triangulation. For example the first regular fine mixed subdivision corresponding to the first regular triangulation is:

$$\{ \{ \{0, 1, 2\} + \{3\} + \{5\} \}, \{ \{0, 2\} + \{3, 4\} + \{5\} \}, \{ \{1, 2\} + \{3\} + \{5, 6\} \}, \\ \{ \{2\} + \{3, 4\} + \{5, 6\} \}, \{ \{2\} + \{3, 4\} + \{6, 7\} \}, \{ \{2\} + \{4\} + \{5, 6, 7\} \} \}$$

each cell of the subdivision correspond to a simplex of the triangulation. Note that all cells except the first and the last one are mixed.

At the next step we check the mixed cell configurations with respect to mixed cells. In this example we take 26 mixed cell configurations which means that all equivalence classes have one element each.

Applying theorem 1.3.4 to the mixed subdivisions we take the symbolic *extreme* terms. This is a list of the symbolic terms together with the set of the subdivisions which produce the corresponding term (i.e. R-equivalent subdivisions)

$$\begin{array}{ll} C_{02}^2 C_{10}^2 C_{20}^2 & \{0, 1, 2, 3, 4, 12, 13, 14\} \\ C_{00}^2 C_{10}^2 C_{22}^2 & \{7, 8, 9, 10, 11, 23, 24, 25\} \\ C_{00} C_{02} C_{11}^2 C_{21}^2 & \{5, 6, 18, 19\} \\ C_{20} C_{22} C_{01}^2 C_{11}^2 & \{16, 17, 20, 21\} \\ C_{00} C_{01} C_{21} C_{22} C_{11}^2 & \{22\} \\ C_{01} C_{02} C_{20} C_{21} C_{11}^2 & \{15\} \end{array}$$

So, the support of $N(R)$ with respect to the symbolic terms $\{C_{00}, C_{01}, C_{02}, C_{10}, C_{11}, C_{20}, C_{21}, C_{22}\}$ is

$$\left\{ \begin{array}{l} \{0, 0, 2, 2, 0, 2, 0, 0\} \\ \{1, 0, 1, 0, 2, 0, 2, 0\} \\ \{2, 0, 0, 2, 0, 0, 0, 2\} \\ \{0, 1, 1, 0, 2, 1, 1, 0\} \\ \{0, 2, 0, 0, 2, 1, 0, 1\} \\ \{1, 1, 0, 0, 2, 0, 1, 1\} \end{array} \right.$$

Then we compute the integer points of the Newton polytope of the Resultant using PORTA [TA97] and we take one extra term $\{1, 0, 1, 2, 0, 1, 0, 1\}$

The following polynomial is the Resultant with symbolic terms:

$$c_1 C_{02}^2 C_{10}^2 C_{20}^2 + c_2 C_{00}^2 C_{10}^2 C_{22}^2 + c_3 C_{00} C_{02} C_{11}^2 C_{21}^2 + c_4 C_{20} C_{22} C_{01}^2 C_{11}^2 + \\ c_5 C_{00} C_{01} C_{21} C_{22} C_{11}^2 + c_6 C_{01} C_{02} C_{20} C_{21} C_{11}^2 + c_6 C_{00} C_{02} C_{20} C_{22} C_{10}^2$$

Note that we also have to compute the coefficients c_i to obtain the Resultant.

Let us conclude this example with a figure. In figure 3.1 there is the 1-skeleton of the Secondary polytope of the previous example. Here the regular triangulations are depicted

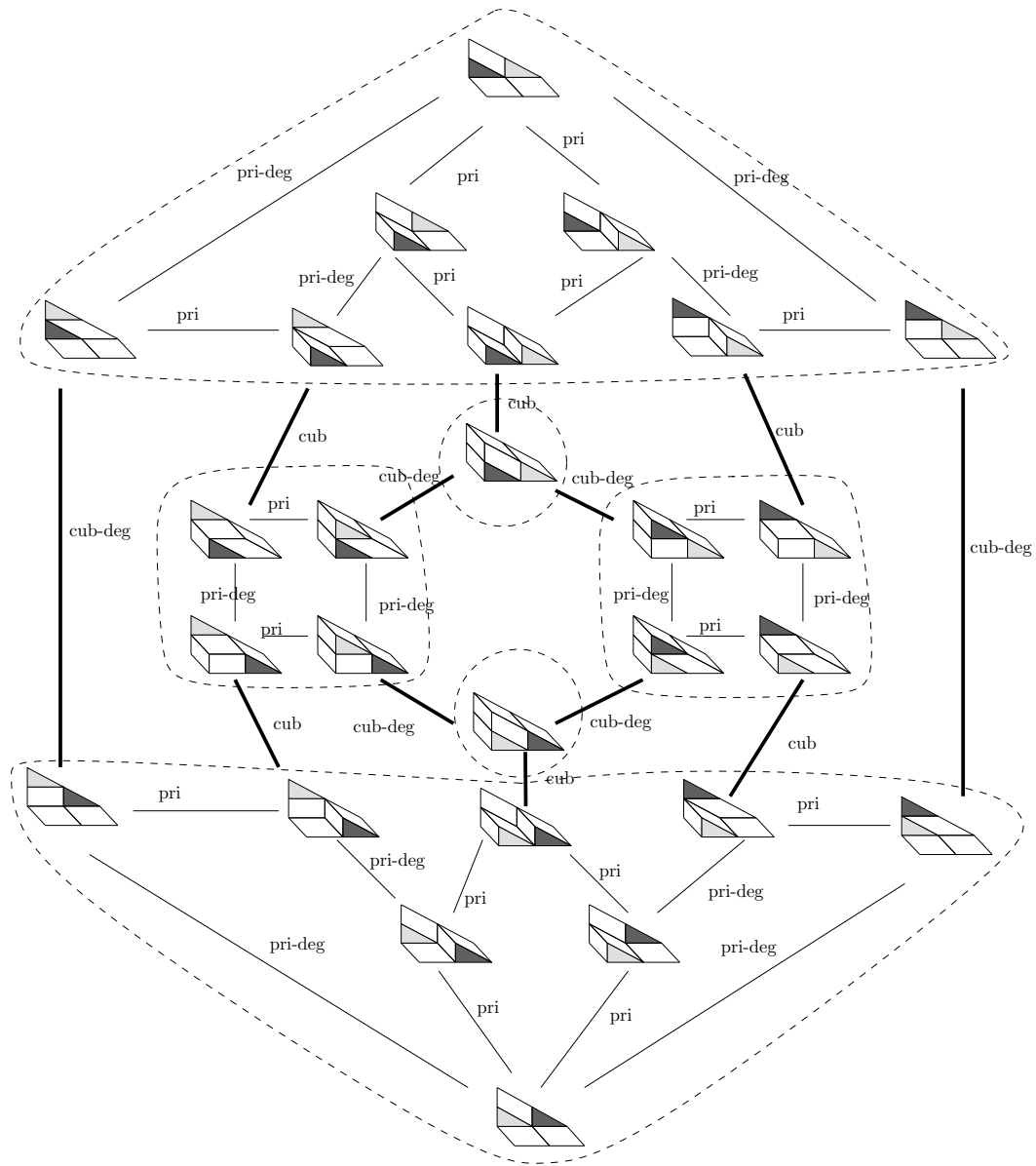


Fig. 3.1: The graph of flips of the point configuration of the circle example. The edges are marked as cub, pri if they correspond to a cubical, (non cubical) flip. They also have a postfix deg if they correspond to a degenerate case.

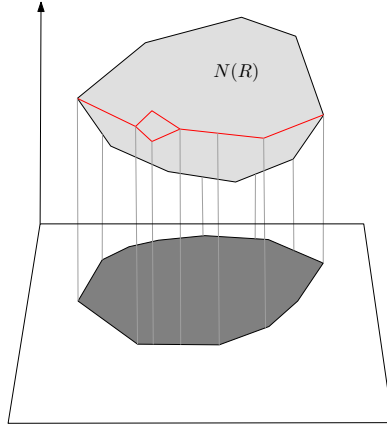


Fig. 3.2: The silhouette of $N(R)$ with respect to a projection.

by their equivalent mixed subdivisions. We can recognize the R-equivalent classes (groups with dashed lines) as well as the edges (flips) that take us from one R-equivalent class to another i.e. the cubical flips (bold edges in the graph). Note that if we consider each R-equivalent class as a vertex and only the bold edges as edges then the resulting graph is the 1-skeleton of the Resultant polytope.

3.4 Conclusions and future work

The first contribution of this thesis is the comparison between the numbers of Secondary, Resultant polytope vertices and i -mixed cell configurations. It is well known [Stu94], [MV97] that $\# \text{ Secondary vertices} \geq \# i\text{-mixed cell configurations} \geq \# N(R) \text{ vertices}$. We show in lemma 2.2.6 that in almost all non trivial cases these inequalities are strict. More interestingly, the first two quantities are much larger than the third one in many cases (see example 2.2.7). However we only know how to enumerate the regular triangulations (see section 1.4) and i -mixed cell configurations (see section 2.1). The computation of $N(R)$ is performed by enumerating either of these and by the above discussion this computation is inefficient.

To overcome this inefficiency we give an algorithmic test for cubical flips in theorem 2.2.2. Cubical flips are defined in [Stu94] and are the flips that connect two subdivisions that correspond to different Resultant vertices. We have also shown in remark 2.2.3 that these flips do not suffice for an algorithm to enumerate the vertices of $N(R)$ because the resulting graph is disconnected.

Another contribution of this thesis is the software that developed for the experiments as well as the experimental results presented in the wiki page [Fis09]. All these would be a starting point for implementations of robust enumeration algorithms of i -mixed cell configurations or Resultant vertices.

As a future work the ultimate goal is the enumeration of the Resultant polytope vertices. To this end we want to study further the fact that $N(R)$ is a Minkowski summand of the

Secondary polytope (see subsection 2.1.1). Additionally, in implicitization we only need to compute a silhouette with respect to a projection of $N(R)$ [Kon06, EKP]. So we would like to construct algorithms that enumerate the vertices the lay on this silhouette (see figure 3.2).

BIBLIOGRAPHY

- [AF92] D. Avis and K. Fukuda. A pivoting algorithm for convex hulls and vertex enumeration of arrangements and polyhedra. *Discrete Comput. Geom.*, 8(3):295–313, 1992.
- [Cha91] B. Chazelle. An optimal convex hull algorithm and new results on cuttings (extended abstract). In *SFCS '91: Proceedings of the 32nd annual symposium on Foundations of computer science*, pages 29–38, Washington, DC, USA, 1991. IEEE Computer Society.
- [DE05] A. Dickenstein and I.Z. Emiris, editors. *Solving Polynomial Equations: Foundations, Algorithms and Applications*. Springer, Berlin, 2005.
- [EFK10] I.Z. Emiris, V. Fisikopoulos, and C. Konaxis. Regular triangularizations and resultant polytopes. In *European Workshop on Computational Geometry (EuroCG)*, pages 137–140, 2010.
- [EK03] I.Z. Emiris and I.S. Kotsireas. Implicit polynomial support optimized for sparseness. In *Intern. CCSA*, pages 397–406, 2003.
- [EK05] I.Z. Emiris and I.S. Kotsireas. Implicitization exploiting sparseness. In R. Jannardan, M. Smid, and D. Dutta, editors, *Geometric and Algorithmic Aspects of Computer-Aided Design and Manufacturing*, volume 67 of *DIMACS*, pages 281–298. AMS, 2005.
- [EKP] Ioannis Z. Emiris, Christos Konaxis, and Leonidas Palios. Computing the newton polytope of specialized resultants. In *Proceeding of the MEGA 2007 conference*.
- [Fis09] V. Fisikopoulos. Implicitization experiments on curves and surfaces wikipedia, 2009. <http://ergawiki.di.uoa.gr/index.php/Implicitization>.

- [GJ00] E. Gawrilow and M. Joswig. polymake: a framework for analyzing convex polytopes. In Gil Kalai and Günter M. Ziegler, editors, *Polytopes — Combinatorics and Computation*, pages 43–74. Birkhäuser, 2000.
- [GKS90] L.J. Guibas, D.E. Knuth, and M. Sharir. Randomized incremental construction of delaunay and voronoi diagrams. In *Proceedings of the seventeenth international colloquium on Automata, languages and programming*, pages 414–431, New York, NY, USA, 1990. Springer-Verlag New York, Inc.
- [GKZ90] I.M. Gelfand, M.M. Kapranov, and A.V. Zelevinsky. Newton polytopes of the classical resultant and discriminant. *Adv. Math.*, 84(2):237–254, 1990.
- [GKZ94] I.M. Gelfand, M.M. Kapranov, and A.V. Zelevinsky. *Discriminants, resultants, and multidimensional determinants*. Birkhäuser, Boston, 1994.
- [IMTI02] H. Imai, T. Masada, F. Takeuchi, and K. Imai. Enumerating triangulations in general dimensions. *Int. J. Comput. Geometry Appl.*, 12(6):455–480, 2002.
- [Kok] Stephen Kokoska. Fifty famous curves, lots of calculus questions, and a few answers. Department of Mathematics, Computer Science, and Statistics, Bloomsburg University.
- [Kon06] C. Konaxis. Triangulations and resultants (master thesis). July 2006. (in Greek).
- [LHTY04] J.A. De Loera, R. Hemmecke, J. Tauzer, and R. Yoshida. Effective lattice point counting in rational convex polytopes. *Journal of Symbolic Computation*, 38(4):1273 – 1302, 2004. Symbolic Computation in Algebra and Geometry.
- [LRS08] J.A. De Loera, J. Rambau, and F. Santos. *Triangulations: Structures and algorithms*. Book manuscript, 2008.
- [Mas95] T. Masada. An algorithm for the enumeration of regular triangulations (master thesis). March 1995.
- [MC00] T. Michiels and R. Cools. Decomposing the secondary Cayley polytope. *Discrete & Computational Geometry*, 23(3):367–380, April 2000.
- [McM71] P. McMullen. The maximum numbers of faces of a convex polytope. *Mathematika*, 17:179–184, 1971.
- [MII96] T. Masada, H. Imai, and K. Imai. Enumeration of regular triangulations. In *SCG '96: Proceedings of the twelfth annual symposium on Computational geometry*, pages 224–233, New York, NY, USA, 1996. ACM.
- [MV97] T. Michiels and J. Verschelde. Enumerating regular mixed-cell configurations. In *Discrete & Computational Geometry*, 1997.

- [PR03] J. Pfeifle and J. Rambau. Computing triangulations using oriented matroids. In *Algebra, Geometry, and Software Systems*, pages 49–75, 2003.
- [Ram02] J. Rambau. TOPCOM: Triangulations of point configurations and oriented matroids. In Arjeh M. Cohen, Xiao-Shan Gao, and Nobuki Takayama, editors, *Mathematical Software—ICMS 2002*, pages 330–340. World Scientific, 2002.
- [San06] F. Santos. Geometric bistellar flips. the setting, the context and a construction. In J. Soria J. L. Varona J. Verdera M. Sanz-Sole, editor, *Proceedings of the International Congress of Mathematicians*, pages 931–962. Eur. Math. Soc., 2006.
- [Stu94] B. Sturmfels. On the Newton polytope of the resultant. *J. Algebraic Comb.*, 3(2):207–236, 1994.
- [SY08] B. Sturmfels and J. Yu. Tropical implicitization and mixed fiber polytopes. In *Software for algebraic geom.*, IMA volumes Math. & Appl., pages 111–131. Springer, 2008.
- [Sym10] SymPy Development Team. *SymPy: Python library for symbolic mathematics*, 2010. <http://www.sympy.org>.
- [TA97] C. Thomas and L. Andreas. PORTA: a collection of routines for analyzing polytopes and polyhedra. 1997.
- [Vaz04] V.V. Vazirani. *Approximation Algorithms*. Springer, March 2004.
- [Wag36] K. Wagner. Bemerkung zum vierfarbenproblem. In *Jahresbericht der Deutschen Mathematiker-Vereinigung 46*, pages 26–32, 1936.
- [Zie95] Günter M. Ziegler. *Lectures on polytopes*. Springer-Verlag, New York, 1995.

- I*-mixed cell configuration, 13
- p*-skeleton, 4
- bistellar flip, 4
- Cayley embedding, 6
- Cayley trick, 6
- chirotope, 9
- circuit, 3
 - oriented, 3
 - signature, 9
- cocircuit, 9
- GKZ-vector, 2
 - I*-mixed, 15
 - mixed, 15
- graph of flips, 4
- link, 3
- lower hull, 2
- Minkowski cell, 5
 - I*-mixed, 13
 - i*-mixed, 5
 - type, 13
- Minkowski sum, 5
- mixed subdivision, 5
- Newton polytope, 7
- polyhedral subdivision, 1
- polynomial system support, 7
- regular subdivision, 2
- Resultant extreme term, 7
- Resultant polytope, 7
- secondary polytope, 2
 - mixed (Ξ), 15
- signature, 8
- sparse resultant, 7
- triangulation, 2
- volume vector, 1

LIST OF FIGURES

1.1	A point set, an invalid subdivisions, a regular polyhedral subdivision, a regular triangulation and a non regular triangulation.	2
1.2	Circuits of dimension 1,2,3 and their corresponding triangulations.	4
1.3	Bistellar flips supported on full dimensional circuits (1,2) and on lower dimensional circuits (3). Link condition not satisfied in (4).	5
1.4	A Minkowski sum of 2 triangles and an edge, one non fine mixed subdivision (the first) and two fine mixed subdivisions (the white cells are mixed and the grey are non mixed).	6
1.5	One picture proof of Cayley trick.	6
1.6	The Newton polytopes of two polynomials.	7
1.7	Chirotopes in 1 and 2 dimensions.	9
1.8	Computing cocircuits [left] and circuits [right] using chirotopes.	9
1.9	[left] Improper intersection detected by a circuit, [right] Interior facet covered by only one simplex.	10
2.1	The classification of i -mixed configurations on mixed subdivisions and the R-equivalent classification on i -mixed configurations.	14
2.2	An illustration of example 2.1.12.	17
2.3	An example of a cubical and two non cubical flips.	19
2.4	Generic flips and degenerate (bold; two edges from different A_i 's are parallel) ones.	20
2.5	An illustration of example 2.2.4. [up-left] The Secondary polytope with the R-equivalent classes (dotted) and the cubical flips (bold). [up-right] The Resultant polytope. [bottom-left] The Secondary polytope with the cubical flips only. The vertices are depicted by the convex hull of the mixed subdivision and the cells that take part on the flip. [bottom-left] The input point sets and the cubical flips.	21

- 3.1 The graph of flips of the point configuration of the circle example. The edges are marked as cub, pri if they correspond to a cubical, (non cubical) flip. They also have a postfix deg if they correspond to a degenerate case. 29
- 3.2 The silhouette of $N(R)$ with respect to a projection. 30